

# A Role for the Lymphotoxin/LIGHT Axis in the Pathogenesis of Murine Collagen-Induced Arthritis<sup>1</sup>

Roy A. Fava,<sup>2\*†</sup> Evangelia Notidis,<sup>‡</sup> Jane Hunt,<sup>\*†</sup> Veronika Szanya,<sup>\*†</sup> Nora Ratcliffe,<sup>\*†</sup> Apinya Ngam-ek,<sup>‡</sup> Antonin R. de Fougerolles,<sup>‡</sup> Andrew Sprague,<sup>‡</sup> and Jeffrey L. Browning<sup>2‡</sup>

A lymphotoxin- $\beta$  (LT $\beta$ ) receptor-Ig fusion protein (LT $\beta$ R-Ig) was used to evaluate the importance of the lymphotoxin/LIGHT axis in the development and perpetuation of arthritis. Prophylactic treatment with the inhibitor protein LT $\beta$ R-Ig blocked the induction of collagen-induced arthritis in mice and adjuvant arthritis in Lewis rats. Treatment of mice with established collagen-induced arthritis reduced the severity of arthritic symptoms and joint tissue damage. However, in a passive model of anti-collagen Ab-triggered arthritis, joint inflammation was not affected by LT $\beta$ R-Ig treatment precluding LT/LIGHT involvement in the very terminal immune complex/complement/FcR-mediated effector phase. Collagen-II and *Mycobacterium*-specific T cell responses were not impaired, yet there was evidence that the overall response to the mycobacterium was blunted. Serum titers of anti-collagen-II Abs were reduced especially during the late phase of disease. Treatment with LT $\beta$ R-Ig ablated follicular dendritic cell networks in the draining lymph nodes, suggesting that impaired class switching and affinity maturation may have led to a decreased level of pathological autoantibodies. These data are consistent with a model in which the LT/LIGHT axis controls microenvironments in the draining lymph nodes. These environments are critical in shaping the adjuvant-driven initiating events that impact the subsequent quality of the anti-collagen response in the later phases. Consequently, blockade of the LT/LIGHT axis may represent a novel approach to the treatment of autoimmune diseases such as rheumatoid arthritis that involve both T cell and Ab components. *The Journal of Immunology*, 2003, 171: 115–126.

The lymphotoxin (LT)<sup>3</sup> system plays crucial roles both in the development of the secondary lymphoid system and in the establishment of ectopic organized lymphoid structures in chronically inflamed sites (1–4). Surface LT (2) is composed of a heteromeric complex of the LT $\alpha$  and LT $\beta$  proteins, and this ligand binds uniquely to the LT $\beta$ R (5). Here, we use the term LT pathway to refer to the biology mediated by the surface LT $\alpha\beta$  ligand via interaction with the LT $\beta$ R. LT $\alpha$  is also secreted as a homotrimeric protein, and human LT $\alpha$  resembles TNF biologically, although the absolute levels are probably quite small relative to TNF. A role for secreted murine LT $\alpha$  homotrimer, which can bind only poorly to TNFR I, has not been unequivocally defined (6). This picture is further complicated by the existence of a second ligand, LIGHT, that binds not only to LT $\beta$ R but also to an additional receptor called herpes virus entry mediator (HVEM) (7).

In the adult immune system, the LT pathway appears to involve communication between subsets of ligand-positive lymphocytes and receptor-positive monocytic, dendritic, and stromal cells (8). In general, this pathway maintains certain microenvironments in the secondary lymphoid organs via the regulation of several specialized reticular stromal cell networks (9, 10). This role has been described best in the context of follicular dendritic cells (FDC). LT, expressed on the surface of B cells, maintains FDCs and potentially non-FDC CD157-positive reticular stromal cells in a fully functional state (9, 11–14). The loss of this maintenance signal results in a rapid collapse of the FDC networks (15, 16). The reticular stromal cells secrete the chemokine B lymphocyte chemoattractant (BLC; CXC ligand 13) which recruits CXCR5-positive B cells and follicular B helper T cells into the follicle (17–20). BLC can induce LT expression in some of these follicular B cells forming a feedback loop that maintains cellular positioning and polarization of the follicle (11). However, exactly how the progression of an Ab-dependent disease is affected by the lack of a functional BLC secreting reticular cell network and how in turn this affects germinal center (GC) formation has not been examined.

Although the coordination of FDC maturation and B cell positioning by the LT system is relatively well understood at least in the spleen, it is likely that aspects of T cell and dendritic cell function are also affected by the LT/LIGHT system (21). Recent *in vivo* studies have magnified this point. Administration of the decoy receptor, LT $\beta$ R-Ig fusion protein (LT $\beta$ R-Ig) blocked disease development in two T cell-based models, experimental colitis and acute rat experimental autoimmune encephalitis (EAE), and eliminated relapses in a chronic relapsing EAE model (22) (J. Gommerman and J. L. Browning, unpublished observations). Expression of a LT $\beta$ R-Ig transgene or pharmacological administration of this agent blocked the emergence of diabetes in the autoimmune nonobese diabetic mouse (23, 24). LT $\beta$ R-Ig inhibited an acute graft vs host response as well as virus-induced CD8 effector cell

\*Department of Veterans Affairs Medical Center, White River Junction, VT 05001;

†Department of Medicine, Dartmouth Medical School, Hanover, NH 03756; and ‡Department of Exploratory Sciences, Biogen, Cambridge, MA 02142

Received for publication February 10, 2003. Accepted for publication April 28, 2003.

The costs of publication of this article were defrayed in part by the payment of page charges. This article must therefore be hereby marked *advertisement* in accordance with 18 U.S.C. Section 1734 solely to indicate this fact.

<sup>1</sup> This work was supported by grants from Veterans Affairs Medical Research, the Hitchcock Foundation, the Arthritis Foundation, and Biogen, Inc. (to R.A.F.).

<sup>2</sup> Address correspondence and reprint requests to Dr. Jeffrey Browning, Biogen, 12 Cambridge Center, Cambridge, MA 02142. E-mail address: jeff\_browning@biogen.com or Dr. Roy A. Fava, Veterans Affairs Medical Center, White River Junction, VT 05001. E-mail address: roy.a.fava@dartmouth.edu

<sup>3</sup> Abbreviations used in this paper: LT, lymphotoxin; LT $\beta$ R-Ig, LT $\beta$  receptor-Ig fusion protein; CIA, collagen-induced arthritis; CII, collagen-II; FDC, follicular dendritic cell; GC, germinal center; ASC, Ab-secreting cell; PNA, peanut agglutinin; GPI, glucose phosphate isomerase; hulgG, human polyclonal IgG; HVEM, herpes virus entry mediator; BLC, B lymphocyte chemoattractant (CXC ligand 13); EAE, experimental autoimmune encephalitis; LN, lymph node; PPD, purified protein derivative.

expansion (25, 26). In the case of LCMV infection, autoimmune prone mice could be rescued by LT $\beta$ R-Ig from a viral shock induced death (26). The effects on lymphocytic choriomeningitis virus-induced CD8 expansion/maturation were paralleled in the ability of LT $\beta$ R-Ig or an anti-LT $\beta$  Ab to block intestinal graft rejection in a CD4 cell-deficient setting (27). A precise description of the relative roles of LIGHT and LT in T cell activation and differentiation has not yet emerged. LIGHT has been implicated in T cell costimulation, and its overexpression as a transgene led to a T cell-based autoimmune disease (7, 28–30). Genetic deletion of the *LIGHT* gene decreased CD8 responses in some settings (31). The efficacy of an anti-LT $\beta$  mAb in both transplant rejection and EAE settings (J. Gommerman and J. L. Browning, unpublished observations) indicate that not all of the effects of LT $\beta$ R-Ig blockade on T cell-based disease models can be attributed simply to the inhibition of *LIGHT*. Therefore, the LT portion of this axis is clearly critical.

A number of models of autoimmune disease rely on the forced recognition of self by immunization with an autoantigen in the presence of adjuvant containing *Mycobacterium tuberculosis*. These rodent models include collagen-induced arthritis (CIA), EAE, and similar models of myasthenia gravis, oophoritis, uveitis, and myocarditis. In this study, we have analyzed the role of the LT/LIGHT axis in the adjuvant-driven CIA model and this represents the first such analysis in a complex T and B cell-driven model of autoimmune disease. Analysis of the role of the LT pathway in autoimmune model systems has been complicated by the linkage of the TNF/LT locus to the MHC which precludes facile genetic deletion in autoimmune prone backgrounds and by the absence of lymph nodes (LN) in LT-deficient animals. To avoid these aspects, we have used a pharmacological inhibitor LT $\beta$ R-Ig and have used the term LT/LIGHT axis to indicate that the activation of LT $\beta$ R by either ligand will be blocked. Administration of the LT $\beta$ R-Ig decoy receptor has mimicked most of the events revealed by genetic dissection, such as blockade of LN development and the disruption of splenic architecture, and therefore it is an effective and validated tool. We report here that blocking the LT/LIGHT axis can significantly alter both the development and the progression of CIA, an animal model with many similarities to human rheumatoid arthritis (32). For comparison, two additional arthritis models were analyzed to help assess the intervention points of the LT/LIGHT axis.

## Materials and Methods

### *Abs and reagents*

A chimeric protein reagent comprised of the extracellular domain of the murine LT $\beta$ R and either a wild-type human IgG1-Fc region or the same molecule incorporating a N297Q mutation that removes the Fc domain glycosylation site have been described elsewhere as have the control proteins and murine TNFR55-Ig (33, 34). A fusion protein of murine HVEM and the human IgG1 Fc domain with the N297Q mutation was prepared. The murine HVEM sequence (independently cloned) that was used in the fusion protein comprised aa 1–206 as defined in ATAR (35). All fusion proteins were prepared from stably transfected Chinese hamster ovary cells and contained <1 endotoxin U per mg of protein. For control proteins, a human LFA-3-human IgG1 fusion protein was used in preliminary experiments and clinical grade polyclonal human IgG (hulG) in later experiments. Similar results were obtained with both control proteins.

### *Induction of arthritis and scoring*

Male DBA/1J mice (The Jackson Laboratory, Bar Harbor, ME) at 7–9 wk of age were immunized with 100  $\mu$ l of a 1:1 v/v emulsion of IFA (Life Technologies, Gaithersburg, MD) and 0.1 M acetic acid containing 100  $\mu$ g of chick type II collagen (CII; Chondrex, Seattle, WA) and 350  $\mu$ g of finely ground heat killed *M. tuberculosis* (Ministry of Agriculture and Fisheries, Weybridge, Surrey, U.K. or Life Technologies). Typically, CII solution was added dropwise to the chilled CFA while a polytron was running to

emulsify. In most experiments, equal amounts of emulsion were injected into the dermis of the tail and into the dermis at the tail base. Mice were boosted on day 21 with 100  $\mu$ g of chick CII in 100  $\mu$ l of 0.05 N acetic acid by i.p. injection, and mice were monitored for the onset of arthritis. Almost all of these experiments were performed at both the VA Medical Center (White River Junction, VT) and in a strict specific pathogen-free facility at Biogen (Cambridge, MA) with similar results. Rat adjuvant arthritis experiments were conducted by treating female Lewis rats (five per group) with 400  $\mu$ g/week LT $\beta$ R-Ig, aglycosyl-LT $\beta$ R-Ig, or hulG. The rats were pretreated for 1 week and then immunized with 0.5 mg of *M. tuberculosis* in 100  $\mu$ l of incomplete adjuvant by injection at the base of the tail. The first signs of arthritis were apparent in the hulG group on day 13. All injections of fusion proteins were i.p.

Mice and rats were scored for severity of arthritis by assigning a score of 0–4 for each limb (0 = no swelling, 1 = swelling in one digit or mild edema, 2 = several digits and moderate swelling, 3 = severe swelling affecting most digits, and 4 = the most severe swelling). Typically, onset of disease occurs over a range of 1–3 wk and affects only one to three paws at a given time point. Affected paws undergo a cycle of increasing swelling maintained for several weeks, followed by decreased swelling and ankylosis. After swelling and inflammation subside in a specific limb, swelling often begins in another previously unaffected limb. This scoring system reflects these decreases of swelling as the disease progresses, as well as the late onset of previously unaffected limbs. A mean arthritis score was determined by summation of the scores of each joint of each mouse divided by the total number of mice or rats in the group. A mean and SEM were determined, and the level of significance was determined by nonparametric methods. The immune complex deposition model of arthritis was performed using BALB/c mice according to the manufacturer's instructions as described previously (36). In brief, 2 mg of the mAb mixture (Chondrex) were injected i.p. on day –3 along with 200  $\mu$ g of human IgG, LT $\beta$ R-Ig, or murine TNFR55-Ig. On day 0, 25  $\mu$ g of LPS were administered i.p., and Ig fusion proteins were injected every third day. All experimental procedures were approved by the Veterans Affairs Administration and the Biogen Institutional Animal Care and Use Committees.

### *Measurement of isotype-specific anti-CII*

Ab titers were quantitated by standard ELISA. Plates with 96 wells (Sarsted, Newton, NC) were coated with chick CII (5  $\mu$ g/ml) in PBS (100  $\mu$ l/well) for 1 h at 37°C and blocked with PBS containing 1% FBS. Serial dilutions of sera were made in PBS with 1% FBS, and 100  $\mu$ l were added to triplicate wells and incubated at 37°C for 1 h. Anti-collagen Abs were revealed with isotype-specific (IgM, IgG1, IgG2a) biotin-conjugated goat anti-mouse antisera (Biosource International, Camarillo, CA) and developed with alkaline phosphatase-streptavidin (Vector Laboratories, Burlingame, CA) and *p*-nitrophenyl phosphate (Sigma-Aldrich, St. Louis, MO) by conventional methods. To normalize plates, each plate included a serial dilution of control mouse serum. For each serum, the dilution that gave an OD reading of 0.2 was determined by extrapolation and plotted.

### *Cell isolations, FACS, and ELISPOT*

For T cell proliferation measurements, pools of draining inguinal LN or spleens were obtained from groups of 5–10 animals. Cell suspensions obtained from LN or spleen cells were resuspended into calcium- and magnesium-free buffers and filtered through nylon filters (BD Biosciences, San Jose, CA). Because we encountered high background proliferation with cells from LT $\beta$ R-Ig-treated animals, we used multiple cell isolation techniques. CD4- or CD8-positive T cells were isolated in some experiments by positive selection with FACS, yielding preparations that were >95% pure (Abs CD4, RM4-4 and CD8, 53-6.7 (BD Biosciences). In other experiments, total T cells were obtained by passage over nylon wool columns, and these preparations were typically 75% pure. In yet other experiments (e.g., Fig. 7B), total LN cells were used, and the amount of proliferation was normalized based on FACS data to correct for varying percentages of T cells in the total population. For ex vivo Ag recall proliferation experiments, draining LN cells were cultured in RPMI medium containing 10% FBS, 2-ME, and HEPES buffer for 4 days and pulsed on the last day for 24 h with [<sup>3</sup>H]thymidine. Denatured pepsin-free T cell proliferation grade CII (Chondrex) or purified protein derivative (PPD; Parke-Davis Pharmaceuticals, Ann Arbor, MI) were used as Ags. Irradiated splenocytes isolated from naive DBA/1 animals were used as APC (300,000 APC with 250,000 T cells per well) in the experiments with purified T cells. ELISA kits for murine IFN- $\gamma$  were obtained from Biosource International. FACS analysis of spleen marginal zone B cell populations was conducted by staining for CD21 (7G8), CD1.1 (1B1) B220 (RA3-6B2), and CD23 (B3B4) (BD Biosciences). B220<sup>high</sup>CD23<sup>low</sup> cells were gated and the CD21<sup>high</sup>CD1<sup>high</sup> marginal zone B cell population was selected for quantitation. Routine

quantitation of T and B cell numbers was performed by FACS using B220 and pan-TCR- $\beta$  Abs.

ELISPOTs of total draining LN and spleen cells were performed as previously described using native chick CII or goat anti-mouse Ig (minimum cross-reactivity; Jackson ImmunoResearch, West Grove, PA) coated MultiScreen-HA plates (Millipore, Bedford, MA) (37). Cells were added to the wells at various concentrations and incubated for 2 h. Captured mouse IgG was detected with alkaline phosphatase-conjugated goat anti-mouse IgG (Southern Biotechnology, Birmingham, AL) and revealed with a 5-bromo-4-chloro-3-indolyl phosphate-nitroblue tetrazolium kit (Vector Laboratories, Burlingame, CA). Errors in most cases were determined by the spread of triplicate determinations using two different cell inputs, i.e., six wells were counted. The data at day 28 were obtained from the analysis of individual animals and then averaged such that data from 12–16 wells were included.

### Histology

Formalin-fixed paraffin sections were decalcified and stained with safranin-O to highlight proteoglycan. Spleens or draining inguinal LN from four to five animals were flash frozen into two OCT blocks with one LN from each animal being present on each block. Cryostat sections 6–10  $\mu$ m thick from each block were acetone fixed and stained with either biotinylated FDC-M2 (Cape Cod Associates, Falmouth, MA) or peanut agglutinin (PNA) coupled to HRP (Sigma-Aldrich) to delineate FDC networks and GCs, respectively. CD4<sup>+</sup> T cells were identified with FITC-labeled anti-CD4 Ab (BD Biosciences) followed by detection with an alkaline phosphatase-coupled anti-FITC Ab (Jackson ImmunoResearch). Bound alkaline phosphatase and HRP activities were visualized using the Histomark Red (Kirkegaard & Perry Laboratories, Gaithersburg, MD) and the Immunopure Metal Enhanced Diaminobenzidine substrate kits (Pierce, Rockford, IL), respectively.

## Results

### Development and progression of CIA is blocked by LT $\beta$ R-Ig

The CIA model is a commonly used mouse model of human rheumatoid arthritis in which disease is induced by immunization of DBA/1 mice with native CII in CFA in the dermis near the tail. After the primary immunization, mice receive a secondary i.p. immunization in the absence of CFA on day 21. When DBA/1 mice were pretreated with LT $\beta$ R-Ig for 2 wk before immunization with CII, clinical signs of arthritis did not develop. In marked contrast, control groups of mice that were either untreated or treated with polyclonal human IgG as a control protein developed clinical signs of disease, although the control protein often caused a slight inhibition of disease (Fig. 1, A and B). Similar results were obtained with 2.4 mg/kg, whereas at 0.6 mg/kg efficacy decreased and onset was delayed 2 wk longer than in control cohorts. Intermediate efficacy was observed previously at 0.2 mg/kg in a CD45RB<sup>high</sup> model of colitis (22). The bioavailability of LT $\beta$ R-Ig in DBA/1 mice was good; i.e., in one study, serum levels of LT $\beta$ R-Ig remained in the 30- to 65- $\mu$ g/ml range with a 60- $\mu$ g/mouse/wk dosing schedule even after 11 weekly injections (data not shown). LT $\beta$ R-Ig was immunogenic, and in BALB/c mice anti-LT $\beta$ R-Ig responses typically occurred at 6–7 wk in animals dosed with 5 mg/kg/wk. We did not determine whether Abs to the drug had limited the effectiveness at the 0.6-mg/kg dose in the CIA model. The marginal zone B cell population in the spleen is very sensitive to LT $\beta$ R-Ig administration and their numbers are a good surrogate marker for the efficacy of the treatment regimen (38). In several experiments, the efficacy of the treatment regimen was evaluated by FACS quantitation of the numbers of marginal zone B cells. Typically, the population of CD1<sup>+</sup>CD21<sup>high</sup>CD23<sup>low</sup> marginal zone B cells is ~10% of the total B220<sup>+</sup> population in DBA/1 mice. A 75–89% decrease was found after 10 days of treatment, and this decrease was maintained through to day 42 (data not shown).

In principle, LT $\beta$ R-Ig could bridge between surface LT- or LIGHT-positive cells and NK or monocytic effector cells. In several instances, such bridging can promote cytolysis of the cell; hence, there can be a more superficial reason for the efficacy of

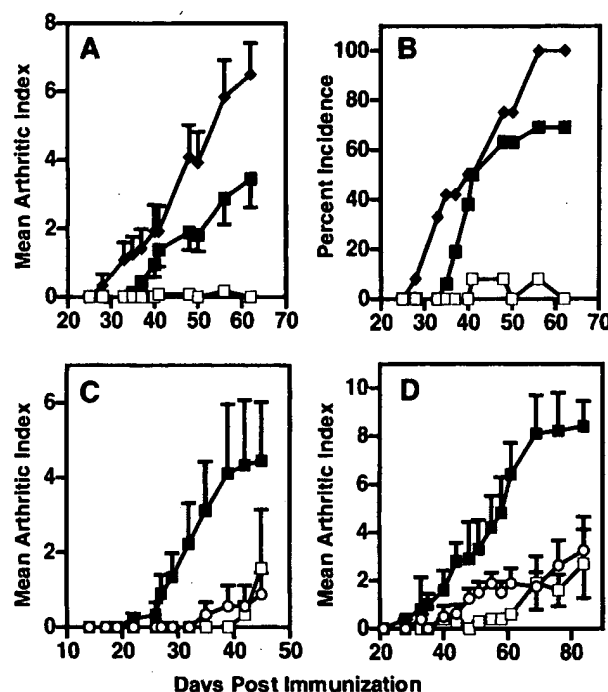


**FIGURE 1.** Treatment with LT $\beta$ R-Ig blocks development of CIA. Mean arthritic indices or percent incidence in CII-immunized DBA/1J mice are shown following various treatments. A and B, Treatment weekly with PBS ( $\blacklozenge$ ), LT $\beta$ R-Ig ( $\square$ ), or human IgG ( $\bullet$ ) at 5 mg/kg (100  $\mu$ g/mouse) started 2 wk before the primary immunization and continued throughout the experiment ( $n = 15$ ); C, as in A, but with control Ig ( $\blacksquare$ ), LT $\beta$ R-Ig ( $\square$ ), or an aglycosyl Fc mutated version of LT $\beta$ R-Ig ( $\circ$ ) ( $n = 10$ ); D, as in A, but with human IgG ( $\blacksquare$ ) and LT $\beta$ R-Ig ( $\square$ ) dosing from day -14 or with dosing with LT $\beta$ R-Ig starting at the same time as the immunization ( $\circ$ ) ( $n = 10$ ). Error bars show the SEM. Similar results were obtained in several experiments of the same design.

chimeric Ig-based inhibitors in vivo models (39). A human IgG1 construct that lacks the glycosylation site in the Fc domain was shown to be incapable of triggering an Ab-dependent cellular cytotoxicity reaction in mice (34). When tested in the CIA model, an aglycosyl construct at a 1- or 5-mg/kg dose was similarly effective in reducing disease scores as was the normal glycosylated LT $\beta$ R-Ig version (Fig. 1C). Therefore, cellular depletion via an Ab-dependent cellular cytotoxicity-type mechanism does not account for the activity of LT $\beta$ R-Ig in amelioration of CIA.

Because several weeks are required in normal mice to elicit the full spectrum of architectural changes in the spleen and a decrease in splenic dendritic cell numbers, two prophylactic treatment schedules were analyzed (21). Either mice were pretreated for 2 wk before immunization to test the effect of architectural disruption on CIA or treatment was initiated several hours before the primary immunization. When treatment was started the same day as the immunization, the incidence of detectable disease was similar to that of control treated mice, yet a much milder disease developed (Fig. 1D).

To determine whether there were subclinical signs of inflammation in joints of mice treated with LT $\beta$ R-Ig from day -14 onwards, histological sections of hind paws of several mice were examined after 80 days of clinical observation. The histological appearance of knee joints and hind paws of mice treated continuously with LT $\beta$ R-Ig was normal without signs of inflammation (data not shown). In contrast, the knee joints and hind paws of human IgG-treated control mice revealed massive neutrophilic and mononuclear cell infiltration, synovial pannus development, loss of articular cartilage, and bone erosions typical of advanced CIA.

Safranin-O staining revealed preservation of the proteoglycan content of articular cartilage in the joints of LT $\beta$ R-Ig-treated animals, whereas joints from control protein-treated animals essentially lacked viable cartilage (Fig. 2). Therefore, treated animals not only had decreased clinical symptoms of disease, but the bone, synovium, and cartilage of the joint were preserved.

#### LT $\beta$ R-Ig inhibits arthritis in established disease

Because LT $\beta$ R-Ig treatment could affect the response of a naive animal to collagen/CFA, we wished to determine whether established disease would be affected. Mice were allowed to progress to a disease score of 4 and then randomized into two treatment groups roughly 5 wk postimmunization. After ~10 days of treatment with LT $\beta$ R-Ig, an ameliorative effect became apparent and was maintained for the next 30 days (Fig. 3). This study was performed twice with similar results. Arthritis in mice treated with the control protein increased to a maximum level of severity significantly higher than that in LT $\beta$ R-Ig treated mice. Blinded histological analysis of the joints from these animals revealed reduced cartilage loss, cellular infiltrates, pannus formation, bone erosion, and ankylosis, indicating that therapeutic treatment effectively blunts the progression of established disease (Table I).

#### Effects of LT $\beta$ R-Ig on the response to CFA

Mice immunized with CII and *M. tuberculosis*-containing adjuvant fail to gain weight postimmunization. This effect results from systemic consequences of the inflammatory response triggered by the *M. tuberculosis*, given that CII Ag is not required for weight loss.

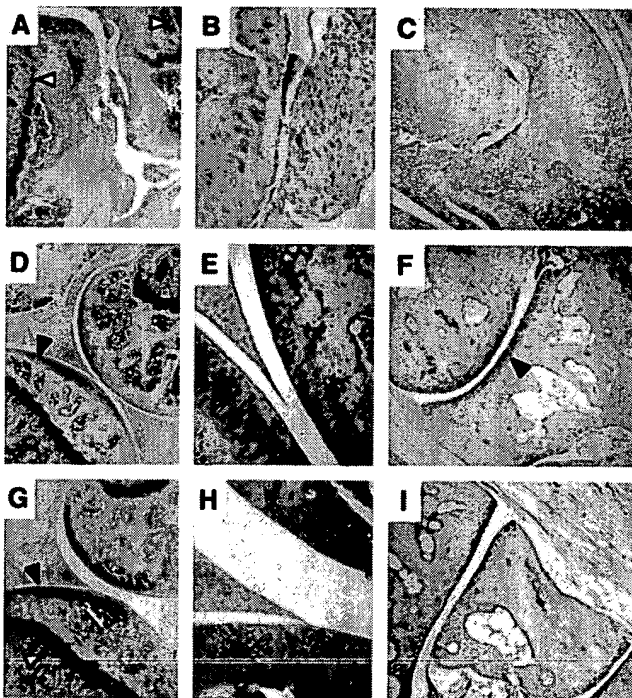


**FIGURE 2.** Safranin-O staining of joints from day 42 mice with CIA to reveal proteoglycan. Collagen-immunized animals were treated with control hulgG (A–C) or LT $\beta$ R-Ig-treated (D–F) from day –14. Healthy non-immunized joints are presented for comparison (G–I). Shown are sections from the knee joints (A, B, D, E, G, and H) and proximal interphalangeal joints (C, F, and I). Closed arrowheads show safranin-O-positive cartilage surfaces, and the open arrowheads delineate safranin-O-positive growth plate epiphyses. A, C, D, F, G, and I are  $\times 50$ ; B, E, and H are  $\times 200$ . Sections are representative of a survey of five joints taken from three different animals per group.

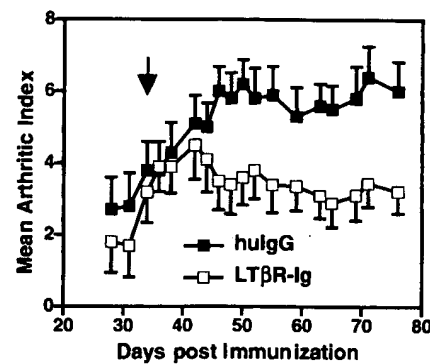


**FIGURE 3.** Treatment with LT $\beta$ R-Ig suppresses established CIA. A. Mice were immunized with chick CII and CFA at day 0 and boosted at day 21. Treatment with 100  $\mu$ g/wk of LT $\beta$ R-Ig ( $\square$ ) or human IgG ( $\blacksquare$ ) was begun 37 days postimmunization (arrow). Mean arthritic scores were calculated and plotted with the SEM. The level of significance between the two curves was determined by the Wilcoxon signed rank test to be  $p = 0.02$  ( $n = 10$ ).

Curiously, LT $\beta$ R-Ig-treated mice that were immunized with either CFA alone or CFA plus CII gained weight more normally, possibly reflecting inhibition of the systemic response to the *M. tuberculosis*-containing adjuvant (Fig. 4). Furthermore, the appearance of the fur of mice during this phase was notably better with LT $\beta$ R-Ig treatment. Extensive necrosis of the tail at the injection site was visible 7–21 days postimmunization. This necrosis is eventually resolved in all groups, although scarring remains as evidenced by kinks in the tails at the injection site. The tails of LT $\beta$ R-Ig-treated animals exhibited considerably reduced necrosis, again indicating a reduced local response to the immunization (data not shown). We suspected that the efficacy of LT $\beta$ R-Ig in CIA hinged on interruption of some fundamental aspect of the adjuvant action of *M. tuberculosis* because an acute rat EAE and an acute allergic myocarditis model were also inhibited by LT $\beta$ R-Ig treatment (J. Gommaman, J. L. Browning, and R. A. Fava, unpublished observations). Arthritis can be induced in susceptible strains of rats by *Mycobacterium* adjuvant alone, and consequently the Lewis rat adjuvant arthritis model was examined. LT $\beta$ R-Ig treatment effectively blunted development of disease in this model. LT $\beta$ R-Ig decreased both incidence and severity in this model and the aglycosyl-LT $\beta$ R-Ig version also reduced disease severity; however, incidence was not significantly impacted in this case (Fig. 5). This observation strongly implicates the LT/LIGHT pathway in the adjuvant component of these models (Fig. 5).

#### LT $\beta$ R-Ig treatment does not affect passive immune complex-triggered joint inflammation

The effector phase of the CIA model can be partially mimicked in a model of murine arthritis wherein a mixture of anti-collagen

**Table I.** Multiple pathological parameters are impacted by therapeutic LT $\beta$ R-Ig treatment of established CIA

Parameter	Disease Score Treatment		$p^*$
	hulgG	LT $\beta$ R-Ig	
Cartilage	1.79	0.91	0.004
Cellularity	1.58	0.87	0.047
Pannus	2.29	1.09	0.001
Bone erosion	2.21	1.13	0.003
Ankylosis	1.71	0.48	0.000

\* ANOVA, 6 mice per group; 20 sections from each paw were analyzed in a blinded format. Analysis was conducted on day 75.

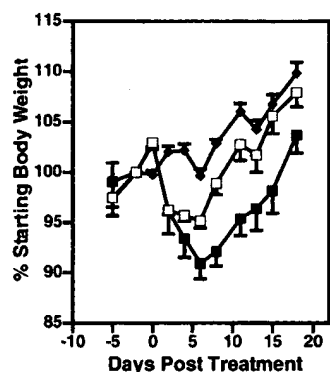


**FIGURE 4.** *Mycobacterium*-driven weight loss in DBA/1 mice is blunted by LT $\beta$ R-Ig treatment. Mice were either naive and untreated ( $\blacklozenge$ ) or injected with *M. tuberculosis* and dosed with either control human IgG ( $\blacksquare$ ) or LT $\beta$ R-Ig ( $\square$ ). Protein treatments were given once weekly starting at day -7 relative to the *M. tuberculosis* injection. Weights of LT $\beta$ R-Ig-treated groups from day 6 onward were significantly improved relative to control human Ig-treated animals (ANOVA  $p < 0.05$ ;  $n = 8$ ).

mAbs is administered and inflammation is initiated by endotoxin injection (40). Presumably, endotoxin-activated monocytes recognize the immune complex deposits in the cartilage and initiate joint destruction. Amplification of this process probably involves the alternate complement pathway and subsequent mast cell involvement (41–43). LT $\beta$ R-Ig treatment did not have an effect in this system (Fig. 6), whereas anti-VLA1 mAb and TNFR55-Ig reduced disease in parallel experiments (36). Because LT $\beta$ R-Ig was not effective in this effector phase setting, the inflammation triggered by immune complex deposition in the joints and endotoxin-induced monocyte and/or granulocyte activation does not involve the LT/LIGHT axis.

#### LT $\beta$ R-Ig treatment and T cell responses to CII

Collagen-specific T cells provide help to the B cell and humoral responses necessary for the development of robust disease. Direct measurement of [ $^3$ H]thymidine incorporation by FACS-sorted CD4 T cells isolated from draining inguinal LNs showed that recall responses to pure denatured pepsin-free collagen were very weak, i.e., about 3000 cpm per 250,000 cells at day 10 post-primary immunization, as has been previously reported (Fig. 7A) (44). This level of response was similar regardless of whether nylon wool-isolated T cells or FACS-sorted CD4 $^+$  T cells were used in the recall cultures. Treatment with LT $\beta$ R-Ig led to increased proliferation by T cells compared with control cells even in the absence of CII Ag and hence the interpretation of any effect on T cell priming was compromised. A similar increase in background

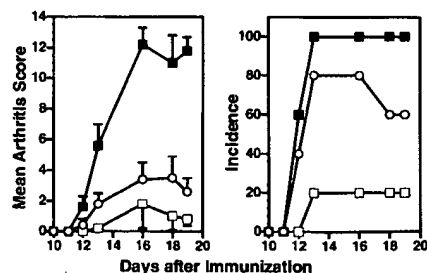


**FIGURE 5.** LT $\beta$ R-Ig blocks adjuvant arthritis in Lewis rats. Disease scores  $\pm$  SEM are shown for animals injected with CFA on day 0 ( $n = 5$ ). Rats were treated once weekly from day -14 with control human Ig ( $\blacksquare$ ), LT $\beta$ R-Ig ( $\square$ ), or aglycosyl-LT $\beta$ R-Ig ( $\circ$ ).

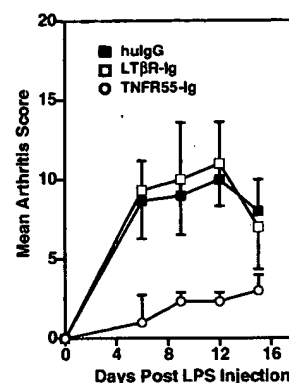


**FIGURE 6.** LT $\beta$ R-Ig does not affect acute anti-CII mAb-driven arthritis. Disease scores  $\pm$  SEM are shown for mice given an anti-CII mAb mixture on day -3 followed by 25  $\mu$ g of LPS on day 0. Control human IgG ( $\blacksquare$ ), LT $\beta$ R-Ig ( $\square$ ), or TNFR55-Ig ( $\circ$ ) was injected (10 mg/kg) on day -3 and every third day thereafter.

proliferation was noted in a study of experimental myasthenia gravis in LT-deficient animals (45). Analysis of spleen cells was also plagued by similar spontaneous T cell proliferation (data not

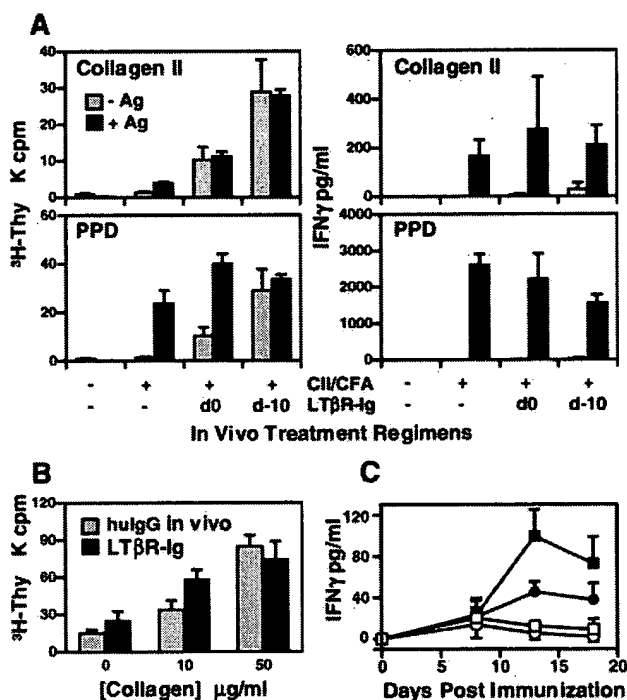


**FIGURE 7.** Effects of LT $\beta$ R-Ig treatment on T cell proliferation. A, CD4 $^+$  T cells from the draining inguinal LN were obtained at day 10 by FACS sorting and stimulated with 50  $\mu$ g/ml chick CII or 10  $\mu$ g/ml PPD as indicated. Left hand graphs, [ $^3$ H]Thymidine ( $^3$ H-Thy) incorporation; right hand graphs, IFN- $\gamma$  production. The wells contained 250,000 T cells and 300,000 irradiated splenic APC. B, Proliferation analysis similar to that in A using total inguinal LN cells (400,000/well) obtained from animals at day 24 (3 days post-booster injection). The counts per minute in the LT $\beta$ R-Ig group were multiplied by a factor of 0.64 to account for the higher proportion of T cells in these LN. Bars,  $\pm$  SE of triplicate wells. Cells from animals treated from day 0 with either control protein ( $\square$ ) and LT $\beta$ R-Ig ( $\blacksquare$ ). C, Serum IFN- $\gamma$  levels were measured after the primary immunization. Animals were injected in the tail with either *Mycobacterium*-containing CFA adjuvant without Ag ( $\circ$ ,  $\square$ ) or with CII Ag ( $\blacksquare$ ,  $\square$ ) and were treated from day -14 with either control protein ( $\square$ ) or LT $\beta$ R-Ig ( $\circ$ ,  $\blacksquare$ ). Sera from four animals per group were analyzed individually, and the average  $\pm$  SE for each time point is plotted. K, Thousands.

shown). In parallel, robust anti-PPD responses were observed in both draining LN and spleen, but LT $\beta$ R-Ig inhibition did not affect the level of [ $^3$ H]thymidine uptake (Fig. 7A). When 200,000 FACS sorted CD8 T cells per well, were analyzed, there was no CII-induced proliferation in the control group or increased background proliferation after in vivo LT $\beta$ R-Ig treatment (data not shown). The effect of LT $\beta$ R-Ig on naive T cell priming and expansion is being analyzed in more tractable systems with stronger T cell responses, e.g., OVA-transgenic TCR- and the myelin basic protein/CFA- and cardiac myosin/CFA-driven systems (J. Gommerman and J. L. Browning, unpublished observations; R. A. Fava, unpublished observations). Quantitation of IFN- $\gamma$  production within these CII recall cultures showed no inhibition by in vivo LT $\beta$ R-Ig treatment (Fig. 7A). Despite the increased background proliferation induced by LT $\beta$ R-Ig treatment, IFN- $\gamma$  secretion in the absence of Ag was not elevated. We speculate that in the transition into in vitro culture conditions, a loss of suppression occurred, resulting in elevated spontaneous proliferation. In the OVA DO.11 TCR-trans-

genic system, in vivo LT $\beta$ R-Ig treatment did not affect cell expansion, but did inhibit the recall proliferation (J. Gommerman, unpublished observations).

Collagen-induced T cell responses were more robust in cells derived from the draining LN at days 24–28, i.e., 3–7 days after the secondary immunization. Cells from LT $\beta$ R-Ig-dosed animals still exhibited some increased background responses; however, there was little inhibition of the recall response by in vivo treatment with LT $\beta$ R-Ig (Fig. 7B). Circulating IFN- $\gamma$  levels in the blood of immunized animals were also quantitated. There was an increase in serum IFN- $\gamma$  levels during the 2 wk following *Mycobacterium* injection. In animals pretreated from day -14 with LT $\beta$ R-Ig, there was a significant decrease in serum IFN- $\gamma$  levels (Fig. 7C). The circulating IFN- $\gamma$  levels may be a surrogate measure of in vivo T cell activity, although monocytes could be a source. Because the general T cell response to CII was relatively weak after the primary immunization, we suspect that the effects on systemic IFN- $\gamma$  are indicative of an effect of LT $\beta$ R-Ig on the

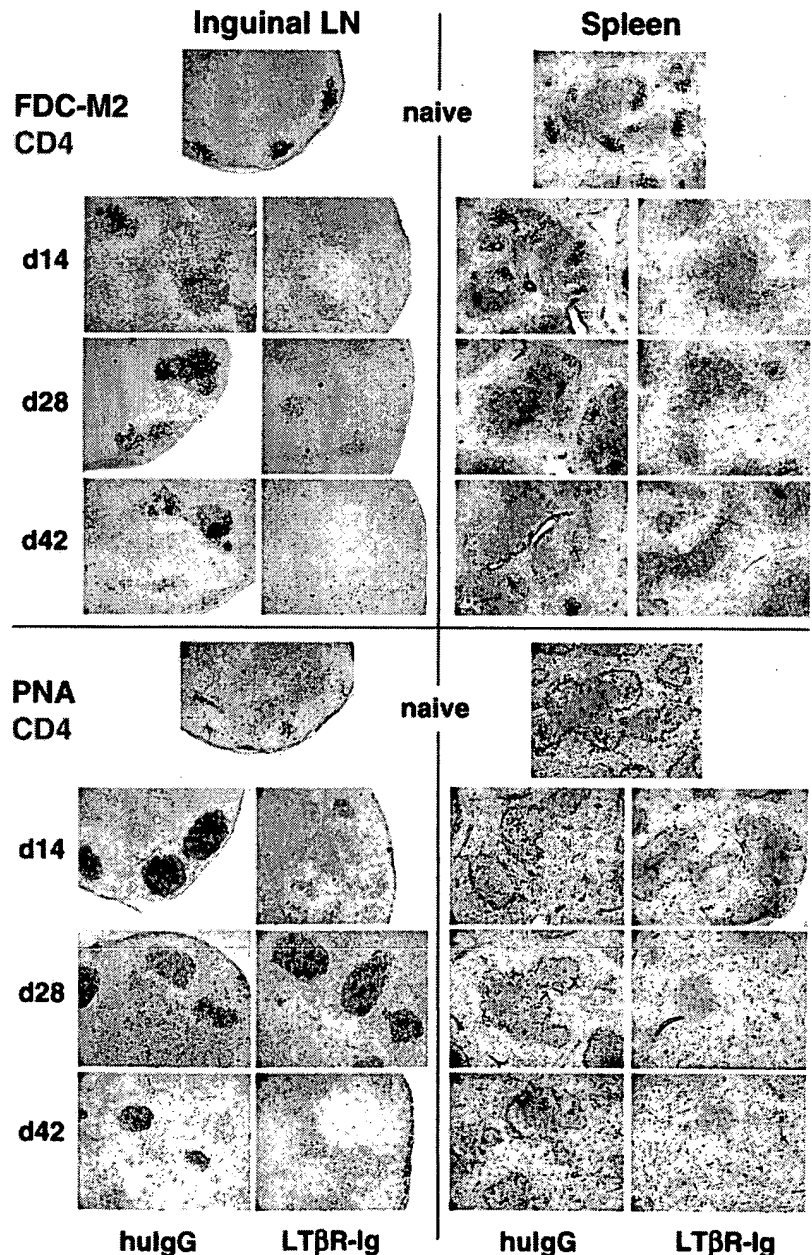


**FIGURE 8.** LT $\beta$ R-Ig treatment affects FDC networks and GC formation in the spleen and draining inguinal LN. Sections labeled naive were obtained from nonimmunized DBA/1 mice; all other sections were derived from CII/CFA-immunized mice that were treated from day 0 with either control hulgG or LT $\beta$ R-Ig. FDC networks were delineated by staining with FDC-M2 (brown) and GCs were stained with PNA (brown). All sections were stained for CD4 (red). Magnification  $\times 100$ ; images are representative of a minimum of four inguinal LN or spleens from four different animals.



adjuvant-induced changes, although direct *in vivo* modulation of T cell responses cannot be excluded.

#### Alterations in lymphoid architecture after LT $\beta$ R-Ig treatment of DBA/1 mice

Changes in splenic architecture after LT $\beta$ R-Ig treatment or genetic ablation of the LT system have been well defined; however, there has not been a description of the effects of LT/LIGHT inhibition on the inflamed LN after immunization with CFA (15, 16). Given the importance of Ig responses in the CIA model, we analyzed the DBA/1 spleens and draining LN throughout days 14 through 42 for the presence of FDC-M2-positive FDC networks and GCs. In the spleen, as expected, FDC networks were readily ablated by LT $\beta$ R-Ig treatment (Fig. 8 and Table II). In general, DBA/1 spleens from naive mice in clean colonies possess zero to four GCs per section as defined by PNA staining. GC formation did not increase substantially in the spleens from most animals injected with CFA/CII; however, the spleens from some animals had many GCs, with 30–90% of the follicles being occupied by GCs. For example, 1 of 9 spleens at days 14–21 had >10 GCs per field, and within one experiment (Table II, Expt. II), only 4 of 16 control Ig-treated spleens collected between days 21 and 42 had high numbers of GCs. We suspect that this variation depends on whether the capillary integrity at the immunization site was grossly breached; therefore, we have not included GC numbers in Table II. It is likely that the spleen does not normally make a major contribution to the primary Ab responses following the standard CIA immunization protocol. Finally, the marginal zone architecture is severely disrupted by LT $\beta$ R-Ig treatment (46), a finding also evident in this study. In addition to GCs, PNA stains the edge of the marginal zone, and this staining was ablated by treatment (Fig. 8).

In the inguinal LN, FDC networks were visible within each follicle. On LT $\beta$ R-Ig treatment of immunized animals, FDC networks had disappeared by day 14 and remained absent for up to

day 42 postimmunization (Fig. 8). Sometimes, very faint networks were visible at day 28, i.e., day 7 after the secondary boost; however, they had disappeared by day 42. The particular networks shown in Fig. 8 were the most prominent ones we were able to find. In other experiments, no networks were visible from days 21 to 42. Typically, small PNA-positive GCs were present at the level of 2–4 per LN section in the absence of immunization. After the primary immunization, prominent GCs were present in the LN from control-treated mice, but their numbers were reduced by LT $\beta$ R-Ig treatment, although there was some variability in the GC content in replicate experiments (Table II). It appears that with the onset of LT $\beta$ R-Ig treatment at day 0, the full effects on GC content occur between 3 and 4 wk later. PNA-positive GCs were clearly found in a complete absence of FDC-M2-positive FDC networks. In all cases examined to date, LT $\beta$ R-Ig treatment eliminated all FDC markers in parallel, i.e., type 1 complement receptor, FDC-M1, FDC-M2, and mucosal addressin cell adhesion molecule expression (15, 16). Whether the inhibitory effects of LT $\beta$ R-Ig treatment on GCs are linked to abortive formation of GCs after the secondary immunization or simply a general decay in the ability to maintain a robust ongoing GC reaction is not clear. In either case, GC formation is impaired by LT $\beta$ R-Ig treatment in the inflamed peripheral LN.

#### Effects of LT inhibition on anti-collagen Ab responses

After CII immunization, animals develop the Abs specific for mouse CII that are the major inducers of joint-specific damage (32,

Table II. Effects of LT $\beta$ R-Ig treatment on the numbers of FDC networks and GCs

Day	Treatment <sup>a</sup>	Mean No. $\pm$ SE		
		Per whole LN section <sup>b</sup>		Per splenic field <sup>c</sup>
		FDC networks	GC	FDC networks
Expt. I				
0	None	3.3 $\pm$ 1.2	0.6 $\pm$ 3.2	44.5 $\pm$ 12.4
14	hulgG	6.3 $\pm$ 2.2	7.2 $\pm$ 2.0	32.3 $\pm$ 6.1
	LT $\beta$ R-Ig	0.0 $\pm$ 0.0	1.8 $\pm$ 3.1	0.0 $\pm$ 0.0
28	hulgG	8.1 $\pm$ 4.0	8.0 $\pm$ 4.4	26.2 $\pm$ 3.7
	LT $\beta$ R-Ig	2.3 $\pm$ 4.0	3.3 $\pm$ 4.2	0.0 $\pm$ 0.0
42	hulgG	6.6 $\pm$ 4.7	5.8 $\pm$ 1.5	24.9 $\pm$ 4.6
	LT $\beta$ R-Ig	0.0 $\pm$ 0.0	0.0 $\pm$ 0.0	0.0 $\pm$ 0.0
Expt. II				
21	hulgG	12.3 $\pm$ 9.8	12.0 $\pm$ 10.4	19.8 $\pm$ 4.3
	LT $\beta$ R-Ig	0.0 $\pm$ 0.0	1.5 $\pm$ 2.4	0.0 $\pm$ 0.0
28	hulgG	4.3 $\pm$ 1.9	3.8 $\pm$ 3.0	20.3 $\pm$ 5.3
	LT $\beta$ R-Ig	0.0 $\pm$ 0.0	0.0 $\pm$ 0.0	0.0 $\pm$ 0.0
35	hulgG	7.7 $\pm$ 9.9	2.7 $\pm$ 4.6	21.8 $\pm$ 5.4
	LT $\beta$ R-Ig	0.0 $\pm$ 0.0	0.0 $\pm$ 0.0	0.0 $\pm$ 0.0
42	hulgG	11.8 $\pm$ 2.9	5.8 $\pm$ 3.4	24.5 $\pm$ 4.4
	LT $\beta$ R-Ig	0.0 $\pm$ 0.0	0.0 $\pm$ 0.0	0.0 $\pm$ 0.0

<sup>a</sup> Treatments were started at day 0 relative to the primary immunization. "None" refers to a DBA/1 spleen that was not injected with CFA/CII and did not receive any protein treatments.

<sup>b</sup> FDC-M2-positive FDCs and all PNA-positive GCs were scored within typically four to five LN sections from four to five animals.

<sup>c</sup> The number of networks per  $\times 50$  field were scored which typically included approximately one-half of a sagittal section of a spleen from a CFA/CII-immunized DBA/1 mouse.

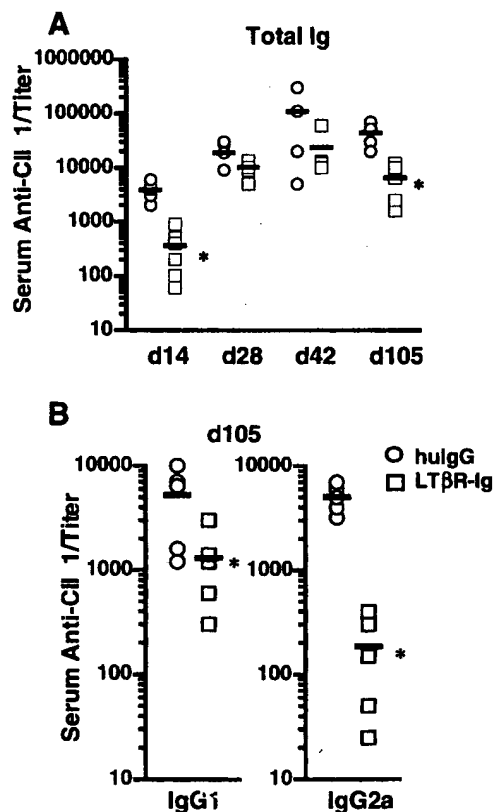


**FIGURE 9.** Inhibition of anti-collagen Ab responses in the sera of mice treated with LT $\beta$ R-Ig from day -14. **A**, Total IgG CII specific Ab titers were analyzed by ELISA on native chicken CII-coated plates during the course of the CIA model. **B**, IgG1 and IgG2a CII-specific CII titers were determined at day 105. Reciprocals of the anti-CII titers are plotted for each LT $\beta$ R-Ig treated ( $\square$ ) and huIgG-treated mouse ( $\circ$ ). Bars, Mean values; \*,  $p < 0.05$ .

Table III. Effects of LT $\beta$ R-Ig treatment on the numbers of anti-CII-secreting B cells in the draining inguinal LN

Day	Treatment <sup>a</sup>	No. of Anti-CII-Secreting Cells <sup>b</sup> ( $\pm$ SE) per		No. of IgG-Secreting Cells <sup>c</sup> ( $\pm$ SE) per	
		10 <sup>6</sup> B cells	LN	10 <sup>6</sup> B cells	LN
Draining inguinal LN					
16	hulG CFA only	1.7 $\pm$ 4.2	7 $\pm$ 16	286 $\pm$ 60	1,086 $\pm$ 229
	LT $\beta$ R-Ig	0 $\pm$ 0	0 $\pm$ 0	216 $\pm$ 48	391 $\pm$ 86
16	hulG	170 $\pm$ 13	761 $\pm$ 141	1,719 $\pm$ 194	7,592 $\pm$ 859
	LT $\beta$ R-Ig	570 $\pm$ 48	1,949 $\pm$ 58	7,358 $\pm$ 272	25,069 $\pm$ 926
28	hulG	161 $\pm$ 63	568 $\pm$ 108	1,104 $\pm$ 109	4,030 $\pm$ 443
	LT $\beta$ R-Ig	75 $\pm$ 56	108 $\pm$ 14	933 $\pm$ 64	660 $\pm$ 44
42	hulG	220 $\pm$ 55	1,159 $\pm$ 287	1,101 $\pm$ 133	5,808 $\pm$ 704
	LT $\beta$ R-Ig	54 $\pm$ 36	31 $\pm$ 21	644 $\pm$ 87	363 $\pm$ 49
Nondraining axillary/brachial LN					
16	hulG	8 $\pm$ 11	9 $\pm$ 12	168 $\pm$ 23	24 $\pm$ 14
	LT $\beta$ R-Ig	69 $\pm$ 30	28 $\pm$ 12	1,030 $\pm$ 292	413 $\pm$ 117
28	hulG	70 $\pm$ 60	40 $\pm$ 6	204 $\pm$ 23	117 $\pm$ 13
	LT $\beta$ R-Ig	77 $\pm$ 79	6 $\pm$ 6	121 $\pm$ 72	9 $\pm$ 5
42	hulG	39 $\pm$ 45	34 $\pm$ 40	254 $\pm$ 67	222 $\pm$ 58
	LT $\beta$ R-Ig	3 $\pm$ 6	0 $\pm$ 1	104 $\pm$ 66	19 $\pm$ 12

<sup>a</sup> Treatments were started at day 0 relative to the primary immunization. All groups were immunized with CII/CFA except the first day 16 entry where only CFA was given.

<sup>b</sup> ELISPOT analyses of CII-specific ASC in total draining inguinal LN and nondraining axillary/brachial LN cells. Errors were determined by the spread of triplicate determinations using two different cell inputs; i.e., six wells were counted. ASC per 10<sup>6</sup> B220 cells were determined using the percentages of B220<sup>+</sup> cells obtained by FACS.

<sup>c</sup> Total IgG-secreting ASC were determined by capture on anti-mouse IgG-coated plates.

44). At day 14, the sera of mice treated with LT $\beta$ R-Ig for 2 wk had reduced total CII-specific titers; yet by day 28, the titers were similar (Fig. 9A). Likewise, little inhibition of total Ig or IgG2a levels was observed in the day 28–42 period in the absence or presence of pretreatment (data not shown), but a significant decrease in titers was observed at later time points, i.e., day 70 and later. The inhibitory effect in the late phase was most pronounced in the anti-CII IgG2a titers (Fig. 8B). IgG1 levels were less affected and IgM titers remained the same (data not shown). In some cases, the titers were determined on autologous mouse CII, and similar trends were observed in the day 28–42 window (data not shown). When LT $\beta$ R-Ig treatment was initiated at day 35 post-primary immunization, i.e., at a time when disease was already manifest as shown in Fig. 3, it was found that the anti-collagen titers of control and LT $\beta$ R-Ig-treated mice were approximately equal at day 63 (data not shown). Thus, it is unlikely that a reduction of serum anti-CII Ab levels is the sole factor in the amelioration of established CIA by LT $\beta$ R antagonism.

In CIA, the draining LN have elevated numbers of Ab-secreting cells (ASC) producing CII specific Abs (37). We quantitated the numbers of such cells in the draining LN by ELISPOT analysis. In accordance with previous observations, we found  $\sim$ 170 CII-ASC cells per 10<sup>6</sup> B220<sup>+</sup> lymphocytes at day 14, and CII-specific ASC were not found in the draining LN after CFA injection without CII Ag (37). This number was roughly maintained through day 42. In contrast, the nondraining axillary and brachial LN contained  $\sim$ 8 ASC per 10<sup>6</sup> B lymphocytes; this value increased to 70 by day 28. Whether this increase reflected dissemination of CII-specific B cells to the nondraining LN or emergence of CIA disease in the forelimbs and hence transport of CII Ag into these LN is not clear. Within the draining LN, CII-specific ASC constituted  $\sim$ 10–15% of the total IgG-secreting cells also in approximate agreement with previous estimates (37). Thus, CIA is similar to the related K/BxN model, where a substantial percentage of ASC in the draining LN are directed against a different autoantigen, i.e., glucose phosphate isomerase (GPI) (47). LT $\beta$ R-Ig treatment initially increased the

frequency at day 14 and then reduced the frequency of CII-ASC 4-fold in the draining LN at days 28–42 (Table III). Why there was a short term increase in ASC in the LN at day 16 is not clear. A similar trend toward decreased CII specific ASC numbers in the nondraining LN was also observed at days 28–42 (Table II). The draining LN in LT $\beta$ R-Ig-treated animals have considerably reduced cell numbers at this stage of disease (days 28–42), therefore taking the decreased cellularity at days 28–42 into account, the total plasma cell numbers per LN were decreased  $\sim$ 40 fold by LT $\beta$ R-Ig treatment in the draining LN. The effects of LT $\beta$ R-Ig on the cell numbers and composition of the LN will be addressed in a separate publication (J. L. Browning and R. A. Fava, manuscript in preparation).

The frequency of ASC in the spleen was  $\sim$ 10-fold lower than that in the draining LN (2.5/10<sup>5</sup> B cells at day 42), and modulation by LT $\beta$ R-Ig treatment was not observed (data not shown). However, due to the large numbers of B cells in a spleen, both the spleen and the pair of draining inguinal LN each contained  $\sim$ 2000 CII-ASC in total at day 42. The four nondraining axillary and brachial LN by comparison contained collectively  $\sim$ 120 CII-specific ASC. Thus, the ability of LT $\beta$ R-Ig treatment to reduce plasma cell numbers occurred during the same period as disease development and may contribute to its efficacy in preventing CIA.

## Discussion

These results demonstrate that LT $\beta$ R-Ig, a dual inhibitor of the LT and LIGHT pathways, blocked the development of disease in both the CIA and adjuvant arthritis models of arthritis and, moreover, reduced established disease in the CIA model. In the CIA model, immunization of mice bearing a permissive H2 haplotype with heterologous (chick) CII and CFA initiates a T-dependent B cell response to autologous (mouse) CII. Both the T and B cell arms of the response are necessary for robust disease development (44). CII-specific Abs are formed, they deposit within the joints, and inflammatory joint destruction is initiated and sustained by immune system recognition of these immune complex deposits (32,



42). The development of a pathological anti-collagen Ab response is T cell dependent (44). The direct contribution of effector T cells to the joint damage is less clear, and once disease has been initiated, ablation of CD4 T cells is ineffective (48). This observation suggests that the late phase is driven by immune complex-triggered events and that CD4 T cells do not contribute substantially. To dissect the effects of LT $\beta$ R-Ig in this system, it is useful to separate the CIA model into the immunological drivers of the autoreactive disease, i.e., T and B cell-mediated events and the effector phase inflammatory mechanisms. The observed efficacy of LT $\beta$ R-Ig when given either prophylactically or therapeutically after disease onset suggests involvement of the LT/LIGHT axis at multiple levels. The lack of substantial disease development when LT $\beta$ R-Ig treatment was given prophylactically most likely reflects intervention at the immunological level, and we discuss this observation first.

The ability of LT $\beta$ R-Ig to prevent CIA without an Fc domain capable of binding Fc $\gamma$ RIII led us to conclude that cellular depletion is not a major component of the efficacy of this chimeric LT $\beta$ R-Ig antagonist. Additional findings consistent with this interpretation include similar data in an acute rat EAE model, the inability of LT $\beta$ R-Ig to impact staphylococcal enterotoxin B-induced T cell expansion in vivo and the ability of LT $\beta$ R-Ig to elicit the full spectrum of altered splenic architecture in Fc $\gamma$ -deficient mice (J. L. Browning, unpublished observations). LT $\beta$ R-Ig blocks both LIGHT and LT activity, and the dissection of these two components has been difficult. We have attempted to assess the role of LIGHT by the use of a LIGHT-specific inhibitor HVEM-Ig. This agent had no efficacy in the CIA model, although in the absence of a positive control system for this reagent, we are still guarded in our interpretation of this result. Furthermore, the antigenicity of a blocking hamster anti-LT $\beta$  mAb prevents its long term usage in the CIA model (J. L. Browning, unpublished observations). Therefore, we cannot definitively delineate between the LT and LIGHT pathways in this setting.

Because the development of disease in both CIA and adjuvant arthritis was blocked and similar observations were made in the acute EAE model<sup>4</sup> and an experimental autoimmune myositis model (R. A. Fava, unpublished observations), it is apparent that *Mycobacterium* adjuvant-driven events are affected by LT $\beta$ R pathway inhibition. The development of a robust autoreactive immune response in these rodent models relies on the ability of the *Mycobacterium* adjuvant to create a favorable microenvironment in the draining LN, thereby promoting an efficient immune response. Current models invoke recognition of pathogen associated molecular patterns by the innate immune system followed by up-regulation of costimulatory molecules on APC and cytokine/chemokine production. In this study, we noticed several effects of LT $\beta$ R-Ig treatment that are consistent with a decreased response to the *Mycobacterium* or downstream sequelae. Weight loss induced by CFA was blunted, possibly reflecting reduced production of cachexia-inducing agents, e.g., TNF. Reduced necrosis at the injection site may be indicative of either a decreased innate immune reaction or reduction of a granuloma or DTH-like response at the site of Ag/adjuvant depot. Markedly decreased levels of circulating IFN- $\gamma$  induced by immunization were also noted with LT $\beta$ R-Ig treatment. These aspects may be consistent with ineffective generation of a conducive microenvironment. Although a defect in the production of IL-12 by DCs from LT-deficient mice has been reported, a precise description of the LT/LIGHT-dependent events

that occur in response to immunization with *Mycobacterium* awaits further work (49).

The efficiency of the immune system resides in large part on the specialized architecture that promotes precisely timed cell-cell encounters in specific locations in lymphoid organs. Some of these architectural and trafficking phenomena are greatly influenced by responses to the mycobacterium in adjuvant and the cytokines that are generated when CFA is deposited with Ag in the dermis. Several studies have described the profound changes following CFA administration that occur in the spleen, e.g. myelopoiesis (50, 51). More recently, a specific and essential role played by the draining LN was revealed in studies on the KBxN model of arthritis, the nonobese diabetic mouse model of diabetes, and in contact hypersensitivity reactions (47, 52, 53). Interestingly, in the case of CIA, disease develops only weakly without CFA, and a spleen is not required (54). LT $\beta$ R-Ig is also capable of blocking inflammatory disease development in models that do not rely on CFA administration, e.g., colitis and diabetes (22–24, 55). Therefore, we favor the view that the microenvironment in the draining LN is the important determinant of the immunological response leading to CIA. The LT system plays an important role in governing the status of the reticular elements in the secondary lymphoid tissues, and these networks are the basic organizers of the local microenvironments (3). For these reasons, we have focused our analyses on the inguinal LN which drain the initial immunization site in CIA.

To dissect the effects of LT $\beta$ R-Ig on T cell vs B cell responses, we attempted to measure CII-induced T cell proliferation, but were hampered for several reasons. First, when in vitro proliferation was measured in a recall format at days 10–12 after the primary immunization with pure pepsin-free collagen, only weak responses are detected (44, 56). Secondly, CD4<sup>+</sup> T cells, whether isolated from the spleen or the draining LN of LT $\beta$ R-Ig-treated CII/CFA immunized animals, proliferated spontaneously at higher levels compared with cells from control-treated animals. Given the very small level of CII-specific T cell stimulation, the addition of a heightened basal proliferation obfuscated the results. We do not yet understand why LT $\beta$ R-Ig treatment induced a heightened basal proliferation rate, although the loss of a suppressive microenvironment may be involved. Likewise, recall responses to collagen following the boost again revealed somewhat higher background proliferation in LT $\beta$ R-Ig-treated cells especially from the draining LN, although now it is clear that a T cell response of CII had occurred during the primary response, even in treated animals. By using a clonotypic marker in related studies, it was found that LT $\beta$ R-Ig treatment did not inhibit T cell priming and expansion in both the DO.11 and OT1 OVA-specific systems, but it did inhibit a T cell recall response in an acute rat EAE model (J. Gommerman, unpublished results; L. LeFrançois, unpublished observations). We currently favor a model whereby maturation into effector T cells is affected by LT pathway inhibitors, but analysis of such activity in the CIA model format is especially problematic.

The generation of pathogenic anti-CII Abs is pivotal to this model and very high levels of these Abs are found in the serum of arthritic mice, i.e., approaching 10% of the total circulating Ig (57). The early anti-CII responses were delayed by treatment of mice with LT $\beta$ R-Ig similar to an earlier report for an anti-keyhole limpet hemocyanin response in LT $\beta$ R-Ig-treated animals (46). From days 21 to 42, only slight or no inhibition was observed. However, substantial inhibition was found at days 70–105 when the full repertoire of affinity matured anti-autologous collagen Abs should be manifested. The effect of LT $\beta$ R-Ig treatment was most pronounced in the IgG2a titer. This reduced level of class switching may reflect the lack of fully functional GC reactions or the reduced

<sup>4</sup> J. Gommerman and J. L. Browning. A role for surface lymphotoxin in experimental autoimmune encephalomyelitis independent of LIGHT. Submitted for publication.

levels of available IFN- $\gamma$ , because IFN- $\gamma$  promotes isotype switching to IgG2a. However, the magnitude of this effect is questionable (58).

The affinity of the anti-CII response was shown to increase 100 fold between the primary and secondary immunizations and this maturation most likely occurs within the GC reaction (59). FDC networks are an essential component of the GC reaction and because these networks can be ablated by LT $\beta$ R-Ig treatment, there is a potential link between treatment and the quality of the anti-CII responses. In both the LN and spleens, FDC networks were eliminated by LT $\beta$ R-Ig treatment with only a few rather sparse networks being observed after the day 21 Ag boost. Similar effects on the networks in both LN and spleens were noted in monkeys (16). GC numbers were also reduced especially in the late phase of the response. Therefore, it is likely that the quality of the secondary phase of the Ab response is impaired by the lack of FDC networks. In an analogous system, the lack of complement receptors led to a reduction in affinity maturation (60). At low doses of nitrophenyl haptenated Ag, both the magnitude of the Ab response and affinity maturation were impaired in mice genetically deficient for either LT $\alpha$  or LT $\beta$ R (61, 62). This inhibition was not observed at a higher dose of Ag indicating that other elements; e.g., B cells can supplant the FDC for presentation purposes. In the case of CII as Ag, it is not clear whether the 100  $\mu$ g of CII protein is a low or a high dose; therefore, the exact impact of altered FDC networks on the quality of the anti-CII response remains unresolved. This problem is complicated by a lack of information on what is required for a pathological anti-CII response. For example, mixtures of anti-collagen mAbs are required to elicit disease when administered passively and a recent analysis of the anti-GPI Abs that mediate chronic arthritis and cause disease in the analogous K/BxN model have highlighted the complex nature of arthritogenic Abs (63, 64). Consequently, according to these studies, the pathogenic potential is likely to be a subtle combination of the magnitude, isotype composition, affinity, and exact epitope specificity of the autoantibody response.

The observed reduction in IgG2a titers could impact the development of CIA by affecting activation of the classical complement arm. Passive immunization of naive rats with anti-CII sera originally implicated the IgG2a subclass of anti-CII Abs in the disease pathology, presumably due to the ability of IgG2a to effectively fix complement. Recent work revealed an obligate role for complement in the development of joint disease in both CIA and GPI models (64, 65). Conversely, IgG1 anti-GPI mAb cocktails were fully active in the passive K/BxN model and efficient activation of the alternate complement pathway by IgG1 Abs underlies this result (64). Moreover, despite severely reduced IgG2a levels in IFN- $\gamma$  receptor-deficient mice, CIA is more severe than in normal mice (50). Perhaps, other aspects of the disease progression can compensate for the lack of IgG2a anti-collagen titers in these particular cases. We speculate that poor quality (e.g., low affinity) anti-CII Abs emerge in the absence of FDC networks, and this aspect is a major component of the efficacy of LT $\beta$ R-Ig in CIA. Further analyses of affinity maturation in this system are ongoing.

ASC that secrete mouse CII-specific Abs are most likely the predominant cells accounting for the anti-CII titers. The percentage of plasma cells found in the total B cell population from LN or spleen was reduced  $\sim$ 4-fold by LT $\beta$ R antagonism at days 28–42. However, because there was an  $\sim$ 5- to 10-fold decrease in total leukocytes per LN in LT $\beta$ R-Ig-treated mice, the number of ASC in the draining LN was  $\sim$ 40-fold lower than in control animals. LT $\beta$ R-Ig treatment similarly reduced cell numbers in Peyer's patches (55), and a detailed description of this effect on inflamed peripheral LN will be presented in a separate publication. The pronounced reduction in ASC numbers suggests that either cells

are trafficking elsewhere or they are not being readily replenished. Given that the GC reaction is a source of both plasma cells and memory B cells, it is possible that the lack of functional GCs at the latter time points contributes to the reduced plasma cell numbers. Why such a decrease is not reflected in the anti-CII Ab titers is somewhat puzzling. It is possible that changes are occurring, but they are obfuscated by the large anti-CII titers present following the primary response and their relatively long serum half-life. The reduced numbers of CII-specific plasma cells at day 42 are likely to account for the reduced Ab titers seen at the later stage, i.e., after 7–8 wk.

LT $\beta$ R-Ig arrested the progression of established CIA disease; this level of efficacy was comparable with the effects of TNF blockade in this model (66). At this point after onset of disease, the immunological drivers of the disease have been established; i.e., T cells capable of providing help to B cells are present and serum anti-collagen titers are already high. Because the titers of anti-collagen Abs were not altered at this point by LT $\beta$ R-Ig treatment and circulating IgG has a relatively long life span in the blood, it is unlikely that modulation of the Ig response can account for the efficacy on established disease. This is an assumption given that one cannot readily monitor the titers of the actual pathological Abs. In the anti-collagen mAb/LPS model of acute arthritis, local immune complex deposits are presumably recognized by LPS-activated macrophages. Studies on the similar anti-GPI Ab model indicate that the effector phase inflammatory cascade is promoted by immune complex interactions with Fc receptors, alternate complement cascade components and mast cell amplification (42, 43). Because arthritis in the passive anti-CII/LPS model was not impacted by LT $\beta$ R-Ig treatment, the more terminal components of the effector phase are likely to be LT/LIGHT independent. Indeed, direct proinflammatory effects of LT $\beta$ R activation on macrophages or granulocytes have not been described. Because the anti-collagen mAb/LPS model is sensitive to inhibitors of TNF- and VLA1-mediated cell trafficking, the activity of LT $\beta$ R-Ig differs from that of a TNF inhibitor at least in this effector phase setting (36). Recent studies do suggest one potential LT $\beta$ R-mediated effect that could account for activity at the established disease level. We have observed that LT $\beta$ R activation in the HT29 epithelial tumor line and in primary endothelial cells resulted in robust induction of the ligands for CXCR3, i.e., monocyte IFN- $\gamma$ -inducible protein, IFN- $\gamma$ -inducible protein-10, and IFN-inducible T cell- $\alpha$  chemoattractant, and we have detected the presence of these chemokines in the serum of mice injected with an LT $\beta$ R agonist mAb (C. Wilson, M. Lukashev, and J. L. Browning, unpublished observations). Because CXCR3 is critical for B, Th1, and NK cell migration into inflamed tissue in several settings, LT $\beta$ R-Ig may blunt trafficking into the inflamed effector sites (67, 68). In accordance with our results, rejection of intestinal transplants appears to involve production of the monocyte IFN- $\gamma$ -inducible protein chemokine, and its synthesis was also blocked by LT inhibition (27). Furthermore, inhibition of IFN- $\gamma$ -inducible protein-10 led to reduced arthritis in the rat adjuvant arthritis model (69).

Here we have shown that antagonism of the LT/LIGHT axis with the LT $\beta$ R-Ig decoy receptor blocked development of arthritis and ameliorated established disease in a rodent model. Thus, modulation of this axis led to inhibition not only of the immunological driver stage, but also the effector phase in established disease. As such, the action of this inhibitor appears to lie at multiple levels. First, there appear to be ill-defined effects on the *Mycobacterium*-induced events that may reflect modulation of the innate immune system. Second, long term Ig production is affected with potential modulation of the quality of the pathogenic Ab response and a very significant reduction in the numbers of ASC. This aspect could

involve the loss of effective presentation and retention of Ag by the FDC networks and abortive GC reactions and/or trafficking aspects of the plasma cells. Lastly, there is the possibility of altered chemokine production within the tissue bed leading to effects at the effector phase although we have not made this link experimentally. Studies of both mouse models and human rheumatoid arthritis have linked the LT system to the generation of ectopic lymphoid centers (3, 4). Therefore, inhibition of this pathway is likely to block the establishment of organized lymphoid microenvironments that could lead to perpetuation of disease. With multilevel involvement, including the maintenance of microenvironments and efficient GC reactions, a dual LT/LIGHT inhibitor may provide a novel approach to modify disease progression in various autoimmune settings.

## Acknowledgments

We thank Randy Noelle, Brian O'Connor, and Paul Guyre, Jennifer Gommerman, Cheryl Nickerson-Nutter, Fabienne Mackay, and Kalpit Vora for valuable assistance and discussions and Jan Farhana for technical assistance.

## References

- Fu, Y. X., and D. D. Chaplin. 1999. Development and maturation of secondary lymphoid tissues. *Annu. Rev. Immunol.* 17:399.
- Ruddle, N. H. 1999. Lymphoid neo-organogenesis: lymphotoxin's role in inflammation and development. *Immunol. Res.* 19:119.
- Luther, S. A., T. Lopez, W. Bai, D. Hanahan, and J. G. Cyster. 2000. BLC expression in pancreatic islets causes B cell recruitment and lymphotoxin-dependent lymphoid neogenesis. *Immunity* 12:471.
- Weyand, C. M., P. J. Kurtin, and J. J. Goronzy. 2001. Ectopic lymphoid organogenesis: a fast track for autoimmunity. *Am. J. Pathol.* 159:787.
- Ware, C. F., T. L. VanArsdale, P. D. Crowe, and J. L. Browning. 1995. The ligands and receptors of the lymphotoxin system. *Curr. Top. Microbiol. Immunol.* 198:175.
- Mackay, F., P. R. Bourdon, D. A. Griffiths, P. Lawton, M. Zafari, I. D. Sizing, K. Miatkowski, A. Ngam-ek, C. D. Benjamin, C. Hession, C. M. Ambrose, W. Meier, and J. L. Browning. 1997. Cytotoxic activities of recombinant soluble murine lymphotoxin- $\alpha$  and lymphotoxin- $\alpha\beta$  complexes. *J. Immunol.* 159:3299.
- Granger, S. W., and C. F. Ware. 2001. Turning on LIGHT. *J. Clin. Invest.* 108:1741.
- Browning, J. L., and L. E. French. 2002. Visualization of lymphotoxin- $\beta$  and lymphotoxin- $\beta$  receptor expression in mouse embryos. *J. Immunol.* 168:5079.
- Vinuesa, C. G., and M. C. Cook. 2001. The molecular basis of lymphoid architecture and B cell responses: implications for immunodeficiency and immunopathology. *Curr. Mol. Med.* 1:689.
- Cyster, J. G., K. M. Ansel, K. Reif, E. H. Ekland, P. L. Hyman, H. L. Tang, S. A. Luther, and V. N. Ngo. 2000. Follicular stromal cells and lymphocyte homing to follicles. *Immunol. Rev.* 176:181.
- Ansel, K. M., V. N. Ngo, P. L. Hyman, S. A. Luther, R. Forster, J. D. Sedgwick, J. L. Browning, M. Lipp, and J. G. Cyster. 2000. A chemokine-driven positive feedback loop organizes lymphoid follicles. *Nature* 406:309.
- Fu, Y. X., G. Huang, Y. Wang, and D. D. Chaplin. 1998. B lymphocytes induce the formation of follicular dendritic cell clusters in a lymphotoxin  $\alpha$ -dependent fashion. *J. Exp. Med.* 187:1009.
- Gonzalez, M., F. Mackay, J. L. Browning, M. H. Kosco-Vilbois, and R. J. Noelle. 1998. The sequential role of lymphotoxin and B cells in the development of splenic follicles. *J. Exp. Med.* 187:997.
- Endres, R., M. B. Alimzhanov, T. Plitz, A. Futterer, M. H. Kosco-Vilbois, S. A. Nedospasov, K. Rajewsky, and K. Pfeffer. 1999. Mature follicular dendritic cell networks depend on expression of lymphotoxin  $\beta$  receptor by radioresistant stromal cells and of lymphotoxin  $\beta$  and tumor necrosis factor by B cells. *J. Exp. Med.* 189:159.
- Mackay, F., and J. L. Browning. 1998. Turning off follicular dendritic cells. *Nature* 395:26.
- Gommerman, J. L., F. Mackay, E. Donskoy, W. Meier, P. Martin, and J. L. Browning. 2002. Manipulation of lymphoid microenvironments in nonhuman primates by an inhibitor of the lymphotoxin pathway. *J. Clin. Invest.* 110:1359.
- Ngo, V. N., H. Korner, M. D. Gunn, K. N. Schmidt, D. S. Riminton, M. D. Cooper, J. L. Browning, J. D. Sedgwick, and J. G. Cyster. 1999. Lymphotoxin  $\alpha\beta$  and tumor necrosis factor are required for stromal cell expression of homing chemokines in B and T cell areas of the spleen. *J. Exp. Med.* 189:403.
- Ngo, V. N., R. J. Cornall, and J. G. Cyster. 2001. Splenic T zone development is B cell dependent. *J. Exp. Med.* 194:1649.
- Breitfeld, D., L. Ohl, E. Kremmer, J. Ellwart, F. Sallusto, M. Lipp, and R. Forster. 2000. Follicular B helper T cells express CXC chemokine receptor 5, localize to B cell follicles, and support immunoglobulin production. *J. Exp. Med.* 192:1545.
- Schaerli, P., K. Willmann, A. B. Lang, M. Lipp, P. Loetscher, and B. Moser. 2000. CXC chemokine receptor 5 expression defines follicular homing T cells with B cell helper function. *J. Exp. Med.* 192:1553.
- Wu, Q., Y. Wang, J. Wang, E. O. Hedgeman, J. L. Browning, and Y. X. Fu. 1999. The requirement of membrane lymphotoxin for the presence of dendritic cells in lymphoid tissues. *J. Exp. Med.* 190:629.
- Mackay, F., J. L. Browning, P. Lawton, S. A. Shah, M. Comiskey, A. K. Bhan, E. Mizoguchi, C. Terhorst, and S. J. Simpson. 1998. Both the lymphotoxin and tumor necrosis factor pathways are involved in experimental murine models of colitis. *Gastroenterology* 115:1464.
- Wu, Q., B. Salomon, M. Chen, Y. Wang, L. M. Hoffman, J. A. Bluestone, and Y. X. Fu. 2001. Reversal of spontaneous autoimmune insulinitis in nonobese diabetic mice by soluble lymphotoxin receptor. *J. Exp. Med.* 193:1327.
- Ettinger, R., S. H. Munson, C. C. Chao, M. Vadeboncoeur, J. Toma, and H. O. McDevitt. 2001. A critical role for lymphotoxin- $\beta$  receptor in the development of diabetes in nonobese diabetic mice. *J. Exp. Med.* 193:1333.
- Tamada, K., K. Shimozaki, A. I. Chapoval, Y. Zhai, J. Su, S. F. Chen, S. L. Hsieh, S. Nagata, J. Ni, and L. Chen. 2000. LIGHT, a TNF-like molecule, costimulates T cell proliferation and is required for dendritic cell-mediated allogeneic T cell response. *J. Immunol.* 164:4105.
- Puglielli, M. T., J. L. Browning, A. W. Brewer, R. D. Schreiber, W. J. Shieh, J. D. Altman, M. B. Oldstone, S. R. Zaki, and R. Ahmed. 1999. Reversal of virus-induced systemic shock and respiratory failure by blockade of the lymphotoxin pathway. *Nat. Med.* 5:1370.
- Guo, Z., J. Wang, L. Meng, Q. Wu, O. Kim, J. Hart, G. He, P. Zhou, J. R. Thistlethwaite, Jr., M. L. Alegre, Y. X. Fu, and K. A. Newell. 2001. Membrane lymphotoxin regulates CD8<sup>+</sup> T cell-mediated intestinal allograft rejection. *J. Immunol.* 167:4796.
- Shaikh, R. B., S. Santee, S. W. Granger, K. Butrovich, T. Cheung, M. Kronenberg, H. Cheroute, and C. F. Ware. 2001. Constitutive expression of LIGHT on T cells leads to lymphocyte activation, inflammation, and tissue destruction. *J. Immunol.* 167:6330.
- Wang, J., J. C. Lo, A. Foster, P. Yu, H. M. Chen, Y. Wang, K. Tamada, L. Chen, and Y. X. Fu. 2001. The regulation of T cell homeostasis and autoimmunity by T cell-derived LIGHT. *J. Clin. Invest.* 108:1771.
- Tamada, K., H. Tamura, D. Flies, Y. X. Fu, E. Celis, L. R. Pease, B. R. Blazar, and L. Chen. 2002. Blockade of LIGHT/TLT $\beta$  and CD40 signaling induces allospecific T cell anergy, preventing graft-versus-host disease. *J. Clin. Invest.* 109:549.
- Scheu, S., J. Alferink, T. Potzel, W. Barchet, U. Kalinke, and K. Pfeffer. 2002. Targeted disruption of LIGHT causes defects in costimulatory T cell activation and reveals cooperation with lymphotoxin  $\beta$  in mesenteric lymph node genesis. *J. Exp. Med.* 195:1613.
- Anthony, D. D., and T. M. Haqqi. 1999. Collagen-induced arthritis in mice: an animal model to study the pathogenesis of rheumatoid arthritis. *Clin. Exp. Rheumatol.* 17:240.
- Browning, J. L., I. D. Sizing, P. Lawton, P. R. Bourdon, P. D. Rennert, G. R. Majeau, C. M. Ambrose, C. Hession, K. Miatkowski, D. A. Griffiths, et al. 1997. Characterization of lymphotoxin- $\alpha\beta$  complexes on the surface of mouse lymphocytes. *J. Immunol.* 159:3288.
- Isaacs, J. D., M. R. Clark, J. Greenwood, and H. Waldmann. 1992. Therapy with monoclonal antibodies: an in vivo model for the assessment of therapeutic potential. *J. Immunol.* 148:3062.
- Hsu, H., I. Solovyyev, A. Colombero, R. Elliott, M. Kelley, and W. J. Boyle. 1997. ATAR, a novel tumor necrosis factor receptor family member, signals through TRAF2 and TRAF5. *J. Biol. Chem.* 272:13471.
- de Fougères, A. R., A. G. Sprague, C. L. Nickerson-Nutter, G. Chi-Rosso, P. D. Rennert, H. Gardner, P. J. Gotwals, R. R. Lobb, and V. E. Koteliansky. 2000. Regulation of inflammation by collagen-binding integrins  $\alpha\beta_1$  and  $\alpha_2\beta_1$  in models of hypersensitivity and arthritis. *J. Clin. Invest.* 105:721.
- Holmdahl, R., C. Bailey, I. Enander, R. Mayer, L. Klareskog, T. Moran, and C. Bona. 1989. Origin of the autoreactive anti-type II collagen response. II. Specificities, antibody isotypes and usage of V gene families of anti-type II collagen B cells. *J. Immunol.* 142:1881.
- Korner, H., T. H. Winkler, J. D. Sedgwick, M. Rollinghoff, A. Basten, and M. C. Cook. 2001. Recirculating and marginal zone B cell populations can be established and maintained independently of primary and secondary follicles. *Immunol. Cell Biol.* 79:54.
- Majeau, G. R., W. Meier, B. Jimmo, D. Kioussis, and P. S. Hochman. 1994. Mechanism of lymphocyte function-associated molecule 3-Ig fusion proteins inhibition of T cell responses: structure/function analysis in vitro and in human CD2 transgenic mice. *J. Immunol.* 152:2753.
- Terato, K., D. S. Harper, M. M. Griffiths, D. L. Hasty, X. J. Ye, M. A. Cremer, and J. M. Seyer. 1995. Collagen-induced arthritis in mice: synergistic effect of *E. coli* lipopolysaccharide bypasses epitope specificity in the induction of arthritis with monoclonal antibodies to type II collagen. *Autoimmunity* 22:137.
- Matsumoto, I., M. Maccioni, D. M. Lee, M. Maurice, B. Simmons, M. Brenner, D. Mathis, and C. Benoist. 2002. How antibodies to a ubiquitous cytoplasmic enzyme may provoke joint-specific autoimmune disease. *Nat. Immunol.* 3:360.
- Ji, H., K. Ohmura, U. Mahmood, D. M. Lee, F. M. Hofhuis, S. A. Boackle, K. Takahashi, V. M. Holers, M. Walport, C. Gerard, et al. 2002. Arthritis critically dependent on innate immune system players. *Immunity* 16:157.
- Lee, D. M., D. S. Friend, M. F. Gurish, C. Benoist, D. Mathis, and M. B. Brenner. 2002. Mast cells: a cellular link between autoantibodies and inflammatory arthritis. *Science* 297:1689.
- Holmdahl, R., M. Andersson, T. J. Goldschmidt, K. Gustafsson, L. Jansson, and J. A. Mo. 1990. Type II collagen autoimmunity in animals and provocations leading to arthritis. *Immunol. Rev.* 118:193.
- Goluszko, E., P. Hjelmstrom, C. Deng, M. A. Poussin, N. H. Ruddle, and P. Christodoss. 2001. Lymphotoxin- $\alpha$  deficiency completely protects C57BL/6

- mice from developing clinical experimental autoimmune myasthenia gravis. *J. Neuroimmunol.* 113:109.
46. Mackay, F., G. R. Majeau, P. Lawton, P. S. Hochman, and J. L. Browning. 1997. Lymphotoxin but not tumor necrosis factor functions to maintain splenic architecture and humoral responsiveness in adult mice. *Eur. J. Immunol.* 27:2033.
  47. Mandik-Nayak, L., B. T. Wipke, F. F. Shih, E. R. Unanue, and P. M. Allen. 2002. Despite ubiquitous autoantigen expression, arthritogenic autoantibody response initiates in the local lymph node. *Proc. Natl. Acad. Sci. USA* 99:14368.
  48. Williams, R. O., and A. Whyte. 1996. Anti-CD4 monoclonal antibodies suppress murine collagen-induced arthritis only at the time of primary immunisation. *Cell. Immunol.* 170:291.
  49. Berger, D. P., D. Nanche, M. T. Crowley, P. A. Koni, R. A. Flavell, and M. B. Oldstone. 1999. Lymphotoxin- $\beta$ -deficient mice show defective antiviral immunity. *Virology* 260:136.
  50. Matthys, P., K. Vermeire, and A. Billiau. 2001. Mac-1<sup>+</sup> myelopoiesis induced by CFA: a clue to the paradoxical effects of IFN- $\gamma$  in autoimmune disease models. *Trends Immunol.* 22:367.
  51. Chu, C. Q., S. Wittmer, and D. K. Dalton. 2000. Failure to suppress the expansion of the activated CD4 T cell population in interferon  $\gamma$ -deficient mice leads to exacerbation of experimental autoimmune encephalomyelitis. *J. Exp. Med.* 192:123.
  52. Rennert, P. D., P. S. Hochman, R. A. Flavell, D. D. Chaplin, S. Jayaraman, J. L. Browning, and Y. X. Fu. 2001. Essential role of lymph nodes in contact hypersensitivity revealed in lymphotoxin- $\alpha$ -deficient mice. *J. Exp. Med.* 193:1227.
  53. Gagnerault, M. C., J. J. Luan, C. Lotton, and F. Lepault. 2002. Pancreatic lymph nodes are required for priming of  $\beta$  cell reactive T cells in NOD mice. *J. Exp. Med.* 196:369.
  54. Wooley, P. H., J. D. Whalen, L. M. Warner, M. K. Losten, and J. M. Chapdelaine. 1989. Type II collagen induced arthritis in mice. V. The role of the spleen cell response in the immune and arthritogenic reaction to type II collagen. *J. Rheumatol.* 16:1192.
  55. Dohi, T., P. D. Rennert, K. Fujihashi, H. Kiyono, Y. Shirai, Y. I. Kawamura, J. L. Browning, and J. R. McGhee. 2001. Elimination of colonic patches with lymphotoxin  $\beta$  receptor-Ig prevents Th2 cell-type colitis. *J. Immunol.* 167:2781.
  56. Vingsbo, C., P. Larsson, M. Andersson, and R. Holmdahl. 1993. Association of pepsin with type II collagen (CII) breaks control of CII autoimmunity and triggers development of arthritis in rats. *Scand J. Immunol.* 37:337.
  57. Holmdahl, R., L. Klareskog, M. Andersson, and C. Hansen. 1986. High antibody response to autologous type II collagen is restricted to H-2q. *Immunogenetics* 24:84.
  58. Stavnezer, J. 1996. Antibody class switching. *Adv. Immunol.* 61:79.
  59. Karlsson, R., J. A. Mo, and R. Holmdahl. 1995. Binding of autoreactive mouse anti-type II collagen antibodies derived from the primary and the secondary immune response investigated with the biosensor technique. *J. Immunol. Methods* 188:63.
  60. Barrington, R. A., O. Pozdnyakova, M. R. Zafari, C. D. Benjamin, and M. C. Carroll. 2002. B lymphocyte memory: role of stromal cell complement and Fc $\gamma$ RIIB receptors. *J. Exp. Med.* 196:1189.
  61. Matsumoto, M., S. F. Lo, C. J. Carruthers, J. Min, S. Mariathasan, G. Huang, D. R. Plas, S. M. Martin, R. S. Geha, M. H. Nahm, and D. D. Chaplin. 1996. Affinity maturation without germinal centres in lymphotoxin- $\alpha$ -deficient mice. *Nature* 382:462.
  62. Futterer, A., K. Mink, A. Luz, M. H. Kosco-Vilbois, and K. Pfeffer. 1998. The lymphotoxin  $\beta$  receptor controls organogenesis and affinity maturation in peripheral lymphoid tissues. *Immunity* 9:59.
  63. Terato, K., K. A. Hasty, R. A. Reife, M. A. Cremer, A. H. Kang, and J. M. Stuart. 1992. Induction of arthritis with monoclonal antibodies to collagen. *J. Immunol.* 148:2103.
  64. Maccioni, M., G. Zeder-Lutz, H. Huang, C. Ebel, P. Gerber, J. Hergueux, P. Marchal, V. Duchatelle, C. Degott, M. van Regenmortel, C. Benoist, and D. Mathis. 2002. Arthritogenic monoclonal antibodies from K/BxN mice. *J. Exp. Med.* 195:1071.
  65. Wang, Y., J. Kristan, L. Hao, C. S. Lenkoski, Y. Shen, and L. A. Matis. 2000. A role for complement in antibody-mediated inflammation: C5-deficient DBA/1 mice are resistant to collagen-induced arthritis. *J. Immunol.* 164:4340.
  66. Williams, R. O., M. Feldmann, and R. N. Maini. 1992. Anti-tumor necrosis factor ameliorates joint disease in murine collagen-induced arthritis. *Proc. Natl. Acad. Sci. USA* 89:9784.
  67. Kunkel, E. J., and E. C. Butcher. 2002. Chemokines and the tissue-specific migration of lymphocytes. *Immunity* 16:1.
  68. Chtanova, T., and C. R. Mackay. 2001. T cell effector subsets: extending the Th1/Th2 paradigm. *Adv. Immunol.* 78:233.
  69. Salomon, I., N. Netzer, G. Wildbaum, S. Schiff-Zuck, G. Maor, and N. Karin. 2002. Targeting the function of IFN- $\gamma$ -inducible protein 10 suppresses ongoing adjuvant arthritis. *J. Immunol.* 169:2685.